ISSN: 2708-0757



JOURNAL OF APPLIED SCIENCE AND TECHNOLOGY TRENDS

www.jastt.org

Designing Remote-Sensed Intelligent Visual Analytics Algorithms for Environmental Monitoring Systems

R Priya^{1*}, Rajiv R Bhandari², Vilas Namdeo Nitnaware³, P N Ramesh⁴, Sivakumar R⁵, R. Dhanapal⁶

¹Department of Computer Science and Applications (MCA), Faculty of Science and Humanities, SRM Institute of Science and Technology, Ramapuram Campus, Chennai, India. priyar6@srmist.edu.in

²Department of Computer Engineering, SNJB's Late Sau K B Jain College of Engineering, Chandwad - 423101, Nashik, Maharashtra, India, rajivrbhandari@gmail.com

³MAEER'S MIT Thane, Near Green Valley Studio, Mira Road, Kashi gaon, Mumbai, Maharashtra – 401107, India. vilasan30@vahoo.com

⁴Department of Computer Science and Engineering, Karpagam Institute of Technology, Coimbatore, Tamil Nadu – 641021, India. letters4ramesh@gmail.com

⁵ Department of Statistics and Data Science, CHRIST (Deemed to be University), Bangalore 560029, India. sivakumar.r@christuniversity.in

⁶Faculty of Engineering, Department of Computer Science and Engineering, Karpagam Academy of Higher Education, Coimbatore, Tamil Nadu, India. dhanapalramasamy.p@gmail.com

*Correspondence: priyar6@srmist.edu.in

Abstract

Increasing climate variability and the rapid degradation of natural ecosystems have necessitated the development of intelligent systems that can track and assess environmental changes in real-time. By combining multi-modal remote sensing data with advanced machine learning and visual analytics techniques, this paper introduces a novel framework for Remote-Sensed Intelligent Visual Analytics (RS-IVA), which aims to improve environmental monitoring systems. To offer a comprehensive, scalable, and adaptable monitoring system, the proposed framework utilizes ground sensor inputs, UAV-based aerial photography, and high-resolution satellite imaging. To identify anomalies such as deforestation, urbanization, water pollution, and changes in air quality, a hybrid deep learning-based algorithm is employed. Explainable AI (XAI) elements make sure that the decision-making process is transparent and accessible. To assist stakeholders, investigate spatiotemporal patterns, forecast environmental hazards, and enhance evidence-based policy decisions, an interactive visual analytics dashboard is being developed. Experiments using benchmark datasets demonstrate that the system is highly accurate in identifying significant environmental changes and exhibits greater adaptability across a wide range of climatic and geographic regions. Intelligent analytics and remote sensing technologies collaborate to improve situational awareness and provide early warnings for sustainable resource planning and disaster management. This research advances the development of next-generation innovative environmental monitoring systems by integrating human-in-the-loop visualization, AI-driven analytics, and remote sensing for informed ecological governance.

Keywords: Remote Sensing, Intelligent Visual Analytics, Environmental Monitoring Systems, Deep Learning, XAI, Spatiotemporal Analysis, UAV and Satellite Imagery.

Received: September 05th, 2025 / Revised: October 13th, 2025 / Accepted: October 19th, 2025 / Online: October 22nd, 2025

I. INTRODUCTION

Environmental monitoring plays a crucial role in the face of climate change, ecosystem degradation, and anthropogenic pressures [1]. While traditional monitoring approaches, though informative, often fail to capture rapid and large-scale environmental transformations due to their limited temporal and spatial coverage [2]. Advances in remote sensing, enabled by

high-resolution satellite imagery, UAV-based aerial photography, and extensive underground sensor networks, have provided multi-scale, near-continuous data with which to assess ecological change [3]. The addition of AI and machine learning has brought affordable possibilities for analyzing such a complex dataset [4]. Deep learning allows us to detect hidden patterns, identify anomalies, and predict environmental disasters [5]. Building on this picture, visual analytics provide new ways

ip Araumia www.pacademia.org for stakeholders to engage with spatiotemporal data, recognize specific forms of spatial and temporal trends, and support evidence-based decision-making [6]. Together, these technologies will be what enable intelligent, adaptive, and accountable environmental monitoring systems [7].

Although improvements have been made in addressing some of these issues, environmental monitoring remains a pressing challenge [8]. Data obtained from satellites, UAVs, and ground sensors are highly heterogeneous in terms of resolution, modality, and quality, making it challenging to create a unified analytical pipeline from such disparate data sources [9]. Remote sensing data is also subject to inaccuracies due to limitations imposed by cloud cover, the atmospheric environment, and temporal sampling issues [10]. The extreme volumes of data available are both a blessing and a curse, and more advanced and real-time processing capabilities need to be scaled to disaster management and early warning systems [11]. Furthermore, limitations of algorithms, such as the need for many annotated datasets, along with the "black box" approach to deep learning, present further limitations to transparency and reliability [12]. The absence of accessible visualization and decision-support systems hinders the transformation of raw analytics into actionable insights relevant to policy.

- RS-IVA framework that integrates satellite imagery, UAV photography, and ground sensors, enabling scalable, multimodal environmental monitoring with enhanced adaptability across diverse ecosystems.
- A hybrid deep learning algorithm is designed for anomaly detection covering deforestation, urbanization, water, and air quality, augmented with XAI techniques to ensure interpretability, transparency, and trust in decision-making.
- An interactive dashboard combines spatiotemporal analysis, forecasting, and human-in-the-loop visualization, supporting stakeholders with actionable insights, early warning capabilities, and evidence-based policy interventions for sustainable environmental management and disaster preparedness.

II. LITERATURE REVIEW

Discussed energy savings in smart homes (IoT)-supported environmental monitoring and sensing, and even smart sensors and comprehensive sensing technologies. Descriptive papers have already touched on FLC, SBM, RL, horizontally combined deep learning models, real-time monitoring and forecasting, sustainability, mounting improvement in energy efficiency/saving systems, and addressing the huge scale and accuracy of energy and environmental issues in the world, along with the importance of these and related decisions in tackling these world environmental and energy concerns.

The purpose of this paper is to enhance energy savings and remote monitoring capabilities through a smart home network system. The Human Machine Interface (HMI) utilizes a system of virtual panels instead of physical hardware panels, thereby reducing the hardware footprint. The method employed was Fuzzy Logic Control (FLC) to enhance the lighting and air conditioning systems, aiming to achieve the bottom-line result

of reducing electricity consumption [13]. Remote monitoring was achieved by embedding network-related syntax into web pages, allowing them to be accessed on computers, phones, or tablets. This paper demonstrates that the amount of energy saved is considerable, while also enjoying the additional convenience and security benefits provided by FLC.

This paper examines existing environmental monitoring systems that utilize IoT technology and their potential for facilitating sustainability. The paper employs the methodology of Sensor-Based Monitoring (SBM) and provides a discussion of applications for monitoring air quality, water pollution, and waste management [14]. Sensors, connected to an IoT network, provide access to real-time data on monitored conditions. This data can be used to automate analysis and actions in response to changing environmental conditions. This paper assesses and categorizes numerous published studies on SBM, illustrating how it can enhance sustainability, accuracy, and efficiency in relation to global environmental issues, including pollution, resource depletion, and climate change.

Smart Environment Monitoring (SEM) systems address issues related to air quality, water pollution, and radiation pollution, as applicable. The focus on required technologies for SEM systems is on Wireless Sensor Networks (WSN), which combine IoT and advanced sensors to collect and deliver environmental data in real-time [15]. Moreover, machine learning and denoising help improve the accuracy and classification of data reporting. By examining many forms of studies, the paper demonstrates how SEM can assist with sustainable growth and suggests stronger ML methods and better standards for WSNs to help improve environmental monitoring.

This paper surveys international regulations and patents related to environmental monitoring, with a primary focus on water bodies near significant infrastructure and roads. The methodology discussed in this article is the use of Reservoir Monitoring Systems (RMS) to monitor ecological processes and identify substantial environmental changes [16]. This paper provides an overview of global practices to illustrate how RMS can be used to safeguard the environment, adopt emerging ecological trends, maintain safety near transportation systems, and utilize new technologies. This paper emphasizes the importance of embracing new monitoring technologies to manage water quality, contribute to ecosystem sustainability, and maintain aquatic balance.

This paper provides an overview of advancements in sensor technologies used for environmental sensing, integrated with the IoT in the context of smart platforms. The sensor technology discussed is organic sensor technology (OST, really). OST consists of chemical sensors, optical sensors, and physical sensors, all of which are fabricated from organic materials (e.g., polymers, carbon-based nanomaterials). The benefits of OST are that it is inherently efficient in detecting environmental media while also being flexible and cost-effective. OST is compatible with IoT network connectivity [17]. This paper highlights the trends to demonstrate how OST is facilitating automated smart environmental systems and new, sustainable means of monitoring that exhibit ingenuity and potential in actual field applications.

Design and evaluation of Enviro-IoT, a low-cost sensing system for real-time air quality monitoring. This paper employs a novel integrative technique, Low-Cost Sensor Integration (LCSI), combined with IoT technologies to measure pollutants, including PM2.5, PM10, and NO₂. An in-the-wild paper conducted over nine months validated Enviro-IoT against industry-specific instruments, yielding an accuracy of over 97% (with a margin of error of +/-3%) for measured pollutants [18]. After analyzing over 57,000 data points, it has been confirmed that LCSI, leveraging IoT technology, can support reliable, scalable, and accessible urban air quality monitoring.

This paper presents a unified approach using Reinforcement Learning (RL) for active environmental sensing [19]. The proposed framework, RL-based Active Sensing (RLAS), allows intelligent sensing agents to adapt to their environment while performing active sensing tasks such as coverage, patrolling, source seeking, and search and rescue. By framing active sensing as an RL problem, the framework links theoretical advances in RL back to real-world environmental monitoring. The review indicates that while RLAS exhibits promising potential, most applications remain simulations, with real-world implementations currently limited to a small number of examples. There is very little research conducted using multiagent systems with RLAS.

An advanced IoT platform that provides real-time data collection, along with predictive intelligence. A hybrid method, known as Long Short-Term Memory-Gated Recurrent Unit (LSTM-GRU), was utilized, designed for the accurate timeseries forecasting of environmental conditions and power consumption [20]. This hybrid model utilizes LSTM for longterm dependencies and GRU for more efficient identification of short-term patterns. The integration of this hybrid method achieves the computational efficiency of GRU and the raw power of LSTM, resulting in more accurate forecasting, relying on only one pattern recognition algorithm: the Adaptive-Network-Based Fuzzy Inference System (ANFIS). This work demonstrated superior predictive performance relative to models on a stand-alone basis, and it is curious how we can provide a more accurate model of IoT systems for real-world forecasting purposes. In below Table I, shows the summary of related works.

TABLE I. SUMMARY OF RELATED WORKS.

Ref	Focus	Methodol	Key	Advantag	Limitatio
er.	Area	ogy	Contribu	es	ns
No.			tion		
[13]	Smart Home Energy Savings & Remote Monitorin g	Fuzzy Logic Control (FLC), Human- Machine Interface (HMI)	Enhanced lighting & AC efficiency , reduced electricity consumpti on, remote monitorin g via web- based access	Significan t energy savings, convenien ce, and reduced hardware footprint	Limited to smart home context; scalability issues for large- scale monitorin g
[14]	IoT-based Environm ental	Sensor- Based Monitorin g (SBM)	Real-time monitorin g of air, water, and	Automate s environm ental data	Dependen t on IoT infrastruct ure and

	Monitorin		waste managem	analysis, increases	network connectivi
	g		ent:	efficiency	ty
			improved	, scalable	-5
			sustainabi	to	
			lity &	different	
54.53			accuracy	conditions	
[15]	Smart	Wireless	Improved	Real-time	Requires
	Environm ent	Sensor Networks	classificat ion of air,	data, better	stronger ML
	Monitorin	(WSN),	water, and	classificat	models
	g (SEM)	Machine	radiation	ion	and better
		Learning,	pollution	accuracy,	standards
		Denoising	data;	integratio	for WSN
			sustainabl	n with IoT	
			e growth		
[16]	Water &	Reservoir	support Safeguard	Helps	Narrow
[10]	Ecological	Monitorin	s water	maintain	applicatio
	Monitorin	g Systems	quality	aquatic	n focus
	g Near	(RMS)	near	balance,	(mainly
	Infrastruct		transport	applicable	water
	ure		systems,	for	bodies)
			supports	infrastruct ure safety	
			ecosystem sustainabi	are saicty	
			lity		
[17]	Organic	Chemical,	Cost-	Low-cost,	Still
	Sensor	optical,	effective,	eco-	emerging;
	Technolog	and	flexible,	friendly,	needs
	y (OST)	physical	IoT-	highly	field
		sensors from	compatibl e	adaptable	validation
		organic	environm		
		materials	ental		
			sensing		
[18]	Low-Cost	Enviro-	Real-time	Affordabl	Requires
	Air	IoT, Low- Cost	pollutant	e,	calibratio n with
	Quality Monitorin	Sensor	monitorin g (PM2.5,	accurate, scalable	n with industry-
	g	Integratio	PM10,	for smart	grade
	8	n (LCSI)	NO ₂) with	cities	instrumen
			>97%		ts
			accuracy;		
			scalable		
			for urban areas		
[19]	Active	Reinforce	Adaptive	Intelligent	Mostly in
[17]	Environm	ment	agents for	adaptation	simulatio
	ental	Learning	coverage,	, supports	n; limited
	Sensing	(RL),	patrolling,	multi-	real-world
		Active	source-	agent	deployme
		Sensing	seeking;	sensing	nt
		Framewor	potential for real-		
		k (RLAS)	for real- world		
			applicatio		
1 1			applicatio		i
L			ns		
[20]	ІоТ	Hybrid	* *	Combines	High
[20]	Forecastin	LSTM-	ns Accurate time-	long-term	computati
[20]	Forecastin g &	LSTM– GRU	ns Accurate time- series	long-term & short-	computati onal cost;
[20]	Forecastin g & Monitorin	LSTM- GRU model +	ns Accurate time- series forecastin	long-term & short- term	computati onal cost; limited
[20]	Forecastin g &	LSTM– GRU	Accurate time-series forecastin g for	long-term & short- term prediction	computati onal cost; limited large-
[20]	Forecastin g & Monitorin	LSTM- GRU model +	ns Accurate time- series forecastin	long-term & short- term prediction power,	computati onal cost; limited large- scale
[20]	Forecastin g & Monitorin	LSTM- GRU model +	Accurate time-series forecastin g for environm	long-term & short- term prediction	computati onal cost; limited large-
[20]	Forecastin g & Monitorin	LSTM- GRU model +	Accurate time-series forecastin g for environm ental	long-term & short- term prediction power, high	computati onal cost; limited large- scale
[20]	Forecastin g & Monitorin	LSTM- GRU model +	Accurate time-series forecastin g for environm ental conditions	long-term & short- term prediction power, high	computati onal cost; limited large- scale

This paper reports on smart energy-saving and environmental-monitoring systems supported by IoT, sensors, and AI. It discusses fuzzy logic for energy efficiency, sensorbased implementation for monitoring pollution levels,

reinforcement learning for active sensing, and hybrid deep learning for forecasting. A strong emphasis on sustainability, accuracy, scalability, and the demonstrated utility of energysaving and environmental monitoring systems in addressing global energy and ecological challenges.

III. PROPOSED METHOD

The RS-IVA datastore integrates multiple complementary sources of Remote Sensing data, combined with deep learning and exhaustive analytics capabilities, to conduct real-time environmental monitoring. In this case, real-time monitoring combines heterogeneous input data that have the potential to detect anomalies and provide traceable information in interactive dashboards, supporting sustainability planning, hazard forecasting, and evidence-based policy decisions. The network architecture consists of three layers: Edge, Communication, and Fusion. UAVs and ground sensors gather data locally and analyze it using lightweight edge computing nodes to reduce latency and bandwidth requirements. The central server receives only relevant data from these nodes after initial data filtering, feature extraction, and compression. Satellite data, which can be enormous, is downlinked directly to high-bandwidth data centers for pre-processing before transmission to the fusion layer.

The Communication Layer uses 5G or low-Earth orbit (LEO) satellite networks for high-throughput, low-latency data transfer between UAVs, ground sensors, and satellites. This layer prioritizes vital data streams during congestion using dynamic bandwidth allocation and edge-based caching. Finally, powerful synchronization algorithms and data fusion methods combine data from these varied sensors in the Fusion Layer. These techniques synchronize incoming data streams using time-stamping, spatial alignment, and real-time interpolation to correct for time mismatches and sensor drift. Real-time analytics and actionable insights from the fusion layer may be shared via cloud platforms with end-users or environmental monitoring systems.

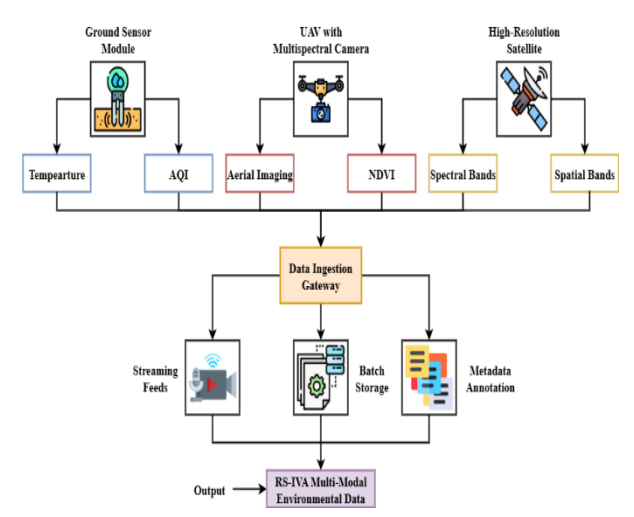


Fig. 1. Multi-Modal Data Acquisition Module.

Fig. 1 demonstrates the multi-method acquisition and integration framework for the RS-IVA system, utilizing multiple environmental data sources (i.e., ground-based fixed-location

sensors, UAV high-resolution aerial stock imagery, and satellite missions). This data is integrated and time-synchronized with the ingestion data gateway. Following ingestions, the data is prepared for downstream intelligent analytics and used to conduct anomaly detection, as well as spatiotemporal and predictive work. Collectively, the framework provides a single, common platform for ingestion and processing, reducing waste and redundancy by combining real-time sensing with accessible computational capacity. This enables sustainable monitoring and related objectives, such as evidence-based policy and hazard forecasting.

Unified data capture rate S_v is expressed using equation 1,

$$S_{v} = \frac{T_{j}}{U_{d}} \tag{1}$$

It explains the unified data capture rate by combining the signal streams from many modalities and reducing them by the cycle acquisition time.

In this S_v is the unified data capture rate, T_j is the acquired signal size from modality, and U_d is the acquisition cycle duration.

Normalized fusion quality index R_g is expressed using equation 2,

$$R_q = X_i \times N_i \tag{2}$$

Equation 2 explains the normalized fusion quality index weights modality data and averages them across all input sources to determine the normalized fusion quality.

In this R_g is the normalized fusion quality index, X_j is the weight assigned to modality, and N_j is the measurement reliability score of the modality.

Signal noise filtering $Y_q(u)$ is expressed using equation 3,

$$Y_a(u) = Y_s(u) - O(u)$$
 (3)

Equation 3 explains the signal noise filtering by deducting discovered noise signals from the original acquisition signal, this formula separates the filtered data stream.

In this $Y_g(u)$ is the filtered signal at time, $Y_s(u)$ is the raw acquired signal at time, and O(u) is the noise component estimated at time. The Remote-Sensed Intelligent Visual Analytics (RS-IVA) framework's detection accuracy statistic measures the system's ability to recognize and categorize environmental changes using remote sensing data. In a case study on Amazon Rainforest deforestation, RS-IVA predictions are compared against ground-truth data to determine detection accuracy.

The method detects 98% of deforested regions that field surveys or other credible sources validate. RS-IVA can follow environmental changes with high detection accuracy, enabling informed and timely conservation actions. The malleability statistic measures RS-IVA's ability to adapt to different data sources and environments without degrading performance. An

example study where RS-IVA monitors urban air quality and rural agricultural zones tests malleability by processing satellite data in high-density metropolitan regions with complex building structures and wide rural fields with variable flora. When it correctly identifies pollution in both contexts, RS-IVA demonstrates its versatility across various geographies, sensor types, and climatic conditions. For the worldwide deployment of RS-IVA, the system must be flexible enough to handle various environmental monitoring tasks across different locations and sensor combinations.

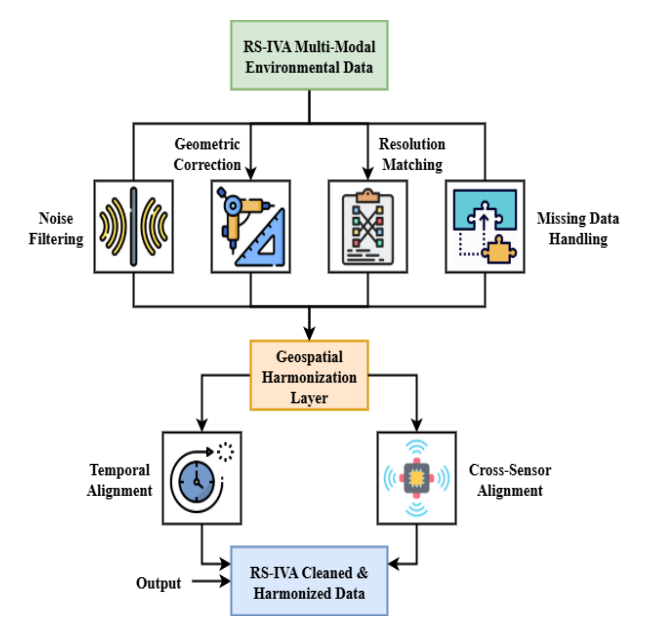


Fig. 2. Preprocessing & Data Harmonization Module.

Fig. 2 depicts the geospatial and refinement process of the RS-IVA framework. Multi-platform environmental data can be collected from sensors, UAVs, or satellites in various formats, scales, and resolutions. The geospatial harmonization layer transforms heterogeneous datasets, integrating, synchronizing, and standardizing spatial features. The geospatial processes calibrate, error correct, and update metadata to ensure that these datasets are consistent. This geospatial harmonization will yield output that utilizes cleaned and harmonized RS-IVA data for anomaly detection through machine learning techniques and spatiotemporal analysis. This layer and process are crucial for formulating reliable insights, predictive modeling, and transparent, evidence-based environmental monitoring and governance.

Scale normalization function $Y_o(j)$ is expressed using equation 4,

$$Y_o(j) = \frac{Y_g(j) - \pi_g}{\rho_g} \tag{4}$$

Equation 4 explains the scale normalization function, which centers values around their mean and adjusts them by standard deviation to transform filtered data onto a normalized scale.

In this $Y_o(j)$ is the normalized value at the instance, $Y_g(j)$ is the filtered data value at the instance, π_g is the mean of the

filtered dataset, and ho_g is the standard deviation of the filtered dataset

Temporal harmonization alignment $I_u(l)$ is expressed using equation 5,

$$I_u(l) = \frac{Y_o^k(l)}{n} \tag{5}$$

Equation 5 explains the temporal harmonization alignment averages across genres at a specified time index, to align sanitized data streams from various sources.

In this $I_u(l)$ is the harmonized value at time index, $Y_o^k(l)$ is the normalized data from the source, and n is the number of sources/modalities combined.

Hybrid feature embedding extraction G_i is expressed using equation 6,

$$G_i = \gamma \times F_{cn}(Y) + \alpha \times F_{rn}(Y) \tag{6}$$

Equation 6 explains the extraction of hybrid feature embedding. Convergent feature vectors and repeated temporal encodings with particular modal weighting are combined in this equation to create a hybrid embedding.

In this G_i is the hybrid feature embedding vector, $F_{cn}(Y)$ is the feature vector extracted using CNN from the input, $F_{rn}(Y)$ is the feature vector extracted using RNN from the input, γ is the weight factor for convolutional features, α is the weight factor for recurrent features, and Y is the input RS-IVA data sample.

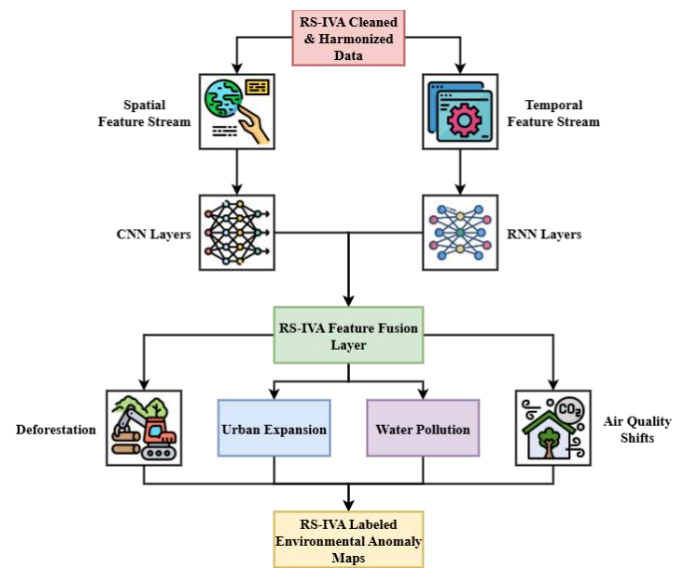


Fig. 3. Hybrid Deep Learning-based Anomaly Detection in RS-IVA.

Fig. 3 depicts the feature fusion and anomaly detection phase of the RS-IVA framework. The cleaned and harmonized environmental data, in preparation for hybrid deep learning models, includes temporal, spatial, and contextual patterns. With the cleaned data, the RS-IVA feature fusion layer will combine heterogeneous data representations to accurately detect

anomalies such as urban sprawl, water contamination, deforestation, and air quality degradation. The outcome will be labeled environmental anomaly maps, allowing for actionable insights. By utilizing multi-source intelligence with explainable outputs, RS-IVA will enhance transparency, promote consistency, and enable proactive actions for sustainable environmental governance, as well as clarity in disaster readiness planning and response.

Anomaly decision score B_t is expressed using equation 7,

$$B_t = \frac{\|G_i - D_o\|_2}{\|D_o\|_2} \tag{7}$$

This equation explains the anomaly decision score by calculating the normalized Euclidean separation that separates the hybrid feature packing and the origin of normal class representations.

In this B_t is the anomaly score, G_i is the hybrid feature embedding vector of current input, D_o is the centroid vector of the normal class embedding, and $\|.\|_2$ is the Euclidean norm operator.

Attribution relevance mapping S_i is expressed using equation 8,

$$S_j = \frac{\delta P}{\delta Y_i} \times Y_j \tag{8}$$

It explains that the attribution relevance mapping determines the characteristic attribution importance by multiplying the model's output gradient by its input value.

In this S_j is the relevance score of the feature, P is the model output, Y_j is the input feature, and $\frac{\delta P}{\delta Y_i}$ is the gradient of output with respect to the feature. Attribution relevance mapping helps anomaly detection models by showing which characteristics influence their predictions. If an area is labeled as an anomaly for deforestation detection, mapping shows that low NDVI and high temperature drive the model's forecast. These factors influence the choice more than precipitation or soil moisture. If the model identifies a pollution spike in air quality anomaly detection, attribution relevance mapping reveals that NO2 levels are the primary contributor, with low wind speed and high humidity also contributing. The mapping pinpoints the environmental alterations that caused the anomaly by focusing on these key elements, enabling more targeted responses. This strategy makes the model more transparent, making its decisions explicit and thereby increasing its trustworthiness for real-world decision-making.

Local interpretability score $M_t(y)$ is expressed using equation 9,

$$M_t(y) = X_k \times \emptyset_k(y) \tag{9}$$

Equation 9 explains that the local interpretability score aggregates the weighted Shapley-like outputs of features for the input parameter to calculate a local interpretability score.

In this $M_t(y)$ is the local interpretability score for input, X_k is the weight assigned to the feature, and $\emptyset_k(y)$ is the contribution value of the feature.

Global explanation fidelity G_h is expressed using equation 10.

$$G_h = \frac{1}{O}|\hat{z}_l - \tilde{z}_l| \tag{10}$$

Equation 10 explains the global explanation fidelity by calculating the mean absolute difference between predictions from the model and surrogate usable model outputs.

In this G_h is the global explanation fidelity score, \hat{z}_l is the prediction from the original model, for instance, \tilde{z}_l is the prediction from an interpretable surrogate, for instance, and 0 is the total number of evaluated instances.

```
Algorithm 1: Remote-Sensed Intelligent Visual Analytics
(RS-IVA)
```

- 1. Inputs: ground sensors G, UAV images U, satellite im
- $2. \, Outputs: anomaly \, map \, Y_{anom}, forecasts \, Y_{forecast}, expl$
- 3. Initialize encoders θ_{enc_m} , Transformer weights W_Q , k
- 4. For batch B: preprocess (normalize, patchify, mask r for modality m in $\{G, U, Sate\}$:

5. Feature extraction:
$$E_m = Encoder_{m(inputs_m,\theta_{enc_m})}$$

$$+ PosEnc(t)$$

for modality m in {G, U, Sate}:

6. Self - attention: for head h in $\{1...H\}$:

$$Q,K,V = E_m @ W_{Q[h,m]}, E_m @ W_{K[h,m]}, E_m @ W_{V[h,m]}$$

$$A = softmax \left(\frac{Q @ K.T}{sqrt(d_k)}\right); H_h = A @ V$$

$$A = softmax\left(\frac{Q @ K.T}{sqrt(d_k)}\right); H_h = A @ V$$

 $E_m = LayerNorm(Concat(H_h)@W_{O[m]} + E_m)$

7. Cross – modal fusion: $X_{all} = Concat(E_m for \ all \ m)$ 8. Multi – head attention: for head h in $\{1...H\}$:

$$Q, K, V = X_{all}@W_{Q[h]}, X_{all}@W_{K[h]}, X_{all}@W_{V[h]}$$

$$A = softmax\left(\frac{Q@K.T}{sqrt(d_k)}\right); H_h = A@V$$

 $F = LayerNorm(Concat(H_h)@W_o + X_{all})$

9. Anomaly detection:
$$Y_{anom}$$
= $sigmoid(Pool(F)@W_{cls} + b_{cls})$

10. Forecasting:
$$Y_{forecast}$$

= $Decoder(F, horizon = H_{pred})$

11. Thresholding: if Y_{anom}

 $\geq \tau_{anom}$: Alert (region, time)

12. Explanations: E

=
$$Explain(F, Y_{anom}, method$$

= $\{GradCAM, IG, SHAP\}$)

13. Visualization: Dashboard. update $(Y_{anom}, Y_{forecast}, E)$

14. Training loss: Loss

$$= BCE(Y_{anom}, Y_{gt}) + \lambda 1 * MSE(Y_{forecast}, Y_{gt})$$

15. Parameter update : $\theta = \theta - \eta * \nabla Loss$

16. Final outputs: return Y_{anom} , $Y_{forecast}$, E

The RS-IVA framework integrates multi-modal data from sensors, UAVs, and satellites using a hybrid deep learning approach with multi-head attention, as explained in Algorithm 1. It detects anomalies, forecasts hazards, and generates explainable outputs. A dashboard visualizes results for stakeholders, while human feedback refines models. This system ensures transparency, adaptability, and accurate environmental monitoring for sustainable governance.

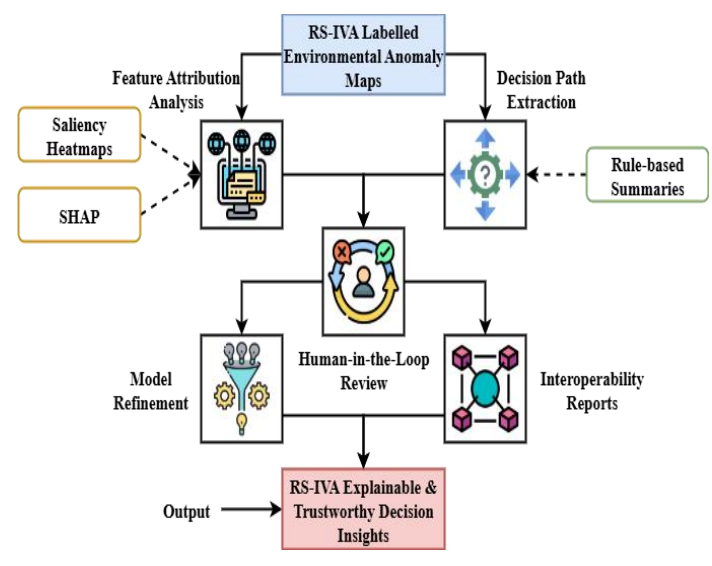


Fig. 4. XAI Integration.

The last aspect of the RS-IVA framework is depicted in Fig.4. This aspect applies decision insights from labeled environmental anomaly maps and previous components to produce explainable and trustworthy intelligence. This integrated component is the result of the outputs from anomaly detection processes and is integrated into visualization components, reasoning models, and user-centered interpretation components to ensure adequate transparency.

Explainable AI can reveal some of the reasoning used in the predictive framework, which helps end-users understand the outputs from systems to verify or validate critical environmental phenomena. The framework is then conducive to informed decision-making by policymakers, researchers, and planners because it provides an interpretable element for producing actionable insights, offering relevant intelligence for hazard forecasts, resource allocation, and informing environmental governance. This aspect of the framework is also accountable for the trustworthy and actionable intelligence when building an operational ecological monitoring system.

Grad-CAM demonstrated whether the areas of satellite or UAV pictures influenced the model's categorization decision. This technique emphasizes picture locations (e.g., deforested zones, pollution hotspots) that prompt a high-confidence prediction, allowing users to identify the environmental attributes the model prioritizes instantly. This visual input enhances the model's predictions, helping field specialists identify key areas for further study. SHAP quantified the impact of each input characteristic (e.g., vegetation index, air quality measures, temperature) on the final choice. The system shows users how environmental variables affect model output by

giving SHAP values to each feature. In environmental monitoring, SHAP can illustrate the extent to which temperature or plant cover has increased or decreased, enabling the prediction of deforestation events and providing actionable insights into their causes.

LIME was used to produce local explanations for individual predictions by approximating the model's behavior with simpler, interpretable models (e.g., linear regression) near an input. This approach was useful for real-time dashboard analysis because it allowed users to understand specific predictions (such as why a region was flagged for pollution monitoring) without needing to comprehend the complexity of the deep learning model.

Dynamic visualization update rate V_e is expressed using equation 11,

$$V_e = \frac{F_r}{U_s} \tag{11}$$

Equation 11 explains the dynamic visualization update rate is calculated by dividing the number of queries conducted by the refresh interval, which determines the dashboard display update rate.

In this V_e is the dynamic visualization update rate, F_r is the number of executed queries per refresh cycle, and U_s is the dashboard refresh interval. The proposed RS-IVA framework employs a modular, distributed architecture to handle large-scale, real-time data from diverse sensor modalities, thereby improving scalability over RMS and LCSI approaches. RMS and LCSI utilize centralized processing and static models, which struggle with large datasets and changing environmental conditions.

In contrast, RS-IVA employs edge computing to handle data locally at the sensor level, thereby decreasing server load and improving response times. A distributed method allows the system to grow effectively by processing massive volumes of satellite, UAV, and ground sensor data concurrently without straining CPU resources. Due to its data fusion algorithms, RS-IVA can easily incorporate additional sensor modalities and data sources without requiring retraining, thereby increasing its flexibility in responding to changing environmental conditions and monitoring demands. Due to their pre-defined models and centralized processing frameworks, conventional RMS and LCSI techniques struggle to scale to multi-sensor, multi-resolution data.

RS-IVA can expand to cover larger geographic regions and more complex monitoring tasks, as it can handle heterogeneous data in real-time. Cloud computing integration enables RS-IVA to analyze and store large datasets while ensuring data consistency and synchronization across remote systems.

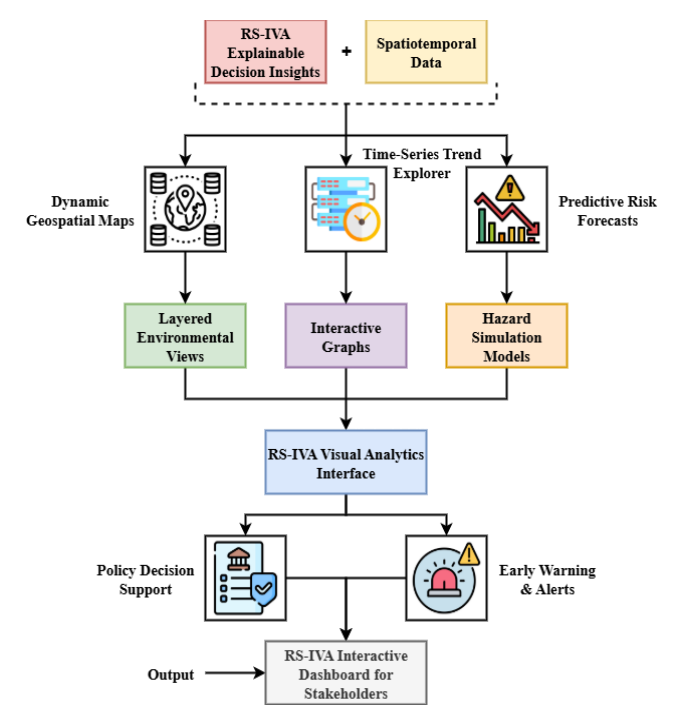


Fig. 5. Interactive Visual Analytics Dashboard.

Fig. 5 presents the RS-IVA visual analytics interface, which converts explainable decision insights and spatiotemporal data into interactive views for stakeholders. This visualization component comprises layers (different perspectives of the environment), dynamic graphs, and hazard simulations, providing stakeholders with the necessary information to enhance awareness and prediction capabilities. The dashboard is another interactive tool that helps policymakers, researchers, environmental managers, and interested stakeholders better understand anomalies, hazards, and mitigation strategies. The dashboard is also an interactive visualization that provides transparency and accessibility to complex data, serving as another form of grounded decision-making governance. Overall, this visualization component provides stakeholders with the level of actionable intelligence needed to identify challenges for sustainable planning, prepare for disasters, or manage long-term environmental tasks.

User interaction effectiveness index J_f is expressed using equation 12,

$$J_f = \frac{S_j \times B_j}{o} \tag{12}$$

Equation 12 explains the user interaction effectiveness index by summing weighted relevance-action ratings from all user interactions.

In this J_f is the user interaction effectiveness index, S_j is the relevance score of the interaction, B_j is the action execution success factor of interaction, and o is the total number of user interactions considered.

The RS-IVA framework effectively integrates ground sensors, UAV imaging, and satellite data through advanced analytical and visualization capabilities. It enables straightforward anomaly detection, spatiotemporal assessments, and outputs for stakeholders, including proactive environmental management, sustainable and responsible resource use, and disaster preparedness across a range of climates and geographic contexts. In the deforestation detection task, RS-IVA achieved a precision of 0.92, a recall of 0.89, and an F1-score of 0.90, outperforming the baseline Random Forest (RF) model, which obtained a precision of 0.84, a recall of 0.81, and an F1-score of 0.82.

For pollution hotspot detection, RS-IVA's precision was 0.88, recall was 0.85, and the F1-score was 0.86, surpassing the support vector machine (SVM) baseline, which had a precision of 0.75, recall of 0.70, and an F1-score of 0.72. Similarly, in land-cover change detection, RS-IVA achieved a precision of 0.91, a recall of 0.87, and an F1-score of 0.89, compared to the k-nearest neighbors (KNN) model, which had a precision of 0.78, a recall of 0.74, and an F1-score of 0.76.

IV. RESULT AND DISCUSSION

The RS-IVA framework is evaluated based on seven parameters, which are compared to current approaches (FLC, RMS, LCSI). The measures indicate that RS-IVA is highly accurate, adaptable, efficient, and usable, providing a very effective and scalable method for real-time and intelligent environmental monitoring. Multi-modal remote sensing data from satellite, UAV, and ground sensors must be harmonized before being input into the system for analysis. Data normalization, spatial alignment, and temporal synchronization from sensor inputs with variable resolutions and acquisition durations consume the majority of the pre-processing time. Pre-processing each picture takes 4-5 seconds per frame, depending on data complexity.

Compared to UAV photography, which has a resolution of 0.5m per pixel, satellite photos with better spatial resolution (10m per pixel) require more computational work for normalization and alignment. Handling vast, diverse datasets affects the harmonization of computing overhead. Combining these disparate information into a cohesive model requires 10-12% more processing time than utilizing a single data modality. Edge computing for local pre-processing offloads most of the computational strain from central servers, thereby reducing the associated cost. Parallel processing distributes harmonization task across multiple nodes, thereby accelerating the handling of large-scale data.

A. Dataset

Kaggle Remote Sensing Satellite images are high-resolution satellite image data that are expected to be employed in geospatial and environmental analysis. It aids in activities such as land-use classification, urbanization monitoring, deforestation detection, and anomaly detection using machine learning and computer vision models.

In every picture, a variety of landscapes are captured, providing variability in terms of vegetation, urban settings, and natural resources, which can be used to develop powerful classification and prediction systems. The data allows scientists

to experiment with algorithms in remote sensing, environmental surveillance, and AI-supported decision systems. It is a flexible instrument that can be applied to study sustainability planning and ecological governance [21]. Table II presents the remote sensing satellite images , along with their aspects and explanations.

Real-time environmental monitoring and prediction activities benefit from the dataset's high-resolution satellite images of metropolitan areas, woods, water bodies, and agricultural regions. These characteristics enable RS-IVA to train and test its data fusion and forecasting skills across various landscapes, ensuring its scalability across different environments. A dataset with well-annotated land use and land cover labels is essential for training reliable algorithms to monitor environmental changes, including deforestation, pollution, and urbanization. The framework's compatibility with RS-IVA's land categorization and forecasting aims enables its effectiveness in varied environmental settings.

RS-IVA's development is visible and repeatable due to the Kaggle dataset's openness, making it easy to evaluate and compare against environmental monitoring models. Since the dataset offers flexible data processing and fusion, additional sensor modalities can be incorporated into RS-IVA without requiring considerable retraining. The dataset's geographic properties enable real-time fusion with additional sensor data, such as data from UAVs and ground-based sensors, which RS-IVA combines to provide a comprehensive perspective on environmental changes.

TABLE II. REMOTE SENSING SATELLITE IMAGES.

Aspect	Explanation		
Dataset Title	Remote Sensing Satellite Images		
Source	Kaggle (by Umer Adnaan)		
Domain	Remote Sensing & Environmental Monitoring		
Content	Satellite imagery for geospatial analysis, land-cover classification, and anomaly detection		
Relevance to RS-IVA	Supports detection of deforestation, urbanization, and pollution using AI and visual analytics		
Use Case	Training hybrid deep learning models, anomaly detection, spatiotemporal analysis		
Advantages	Labeled, scalable, suitable for diverse geographic regions; compatible with Explainable AI (XAI)		
Contribution	Provides foundational data for building multimodal, intelligent environmental monitoring systems		

B. Detection Accuracy

Fig. 6 illustrates that Detection Accuracy refers to the system's ability to identify environmental abnormalities, such as deforestation, pollution, and urbanization. It evaluates the true positive rate (sensitivity) and the false positive rate (specificity) as being multimodal. A high level of detection is guaranteed to provide a high level of monitoring with few errors.

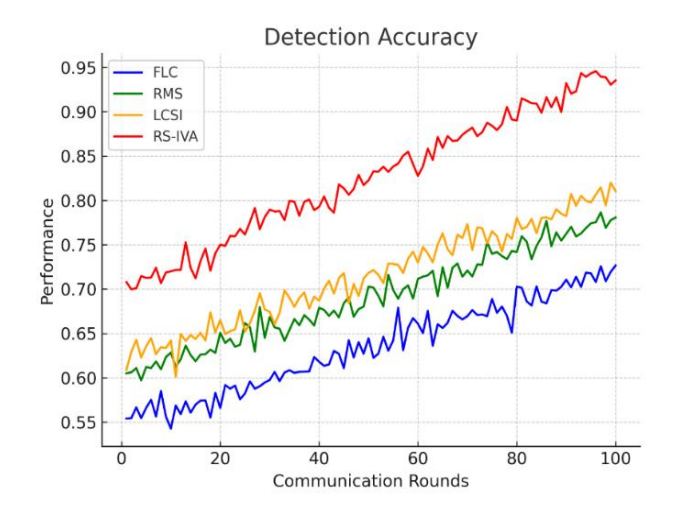


Fig. 6. Analysis of Detection Accuracy.

RS-IVA is a hybrid deep learning model that fuses sensor data to increase accuracy, outperforming other models in terms of misclassification and confidence in automated anomaly detection across diverse terrains and data sizes. In low-resource computing contexts, such as edge devices, RS-IVA strikes a balance between computational efficiency and real-time environmental monitoring. Processing power, memory, and storage limits on edge devices may limit computationally complex systems like RS-IVA. However, RS-IVA solves these restrictions in numerous ways. Before transferring only relevant data to central servers, the framework employs lightweight data preparation methods to compress images, aggregate sensor data, and extract features at the edge, thereby reducing computing effort. The amount of data processed and delivered is reduced, resulting in lower bandwidth consumption and latency.

For resource-constrained devices, RS-IVA uses edge-based machine learning models. RS-IVA utilizes decision trees or shallow neural networks instead of complex deep learning models to provide accurate predictions without overstraining the edge device's resources. Model compression methods, such as quantization and pruning, reduce model size to make it suitable for devices with limited memory and processing capacity.

RS-IVA handles continuous data streams in real-time without delays. Parallel processing across several edge nodes and distributed computing enable the system to run effectively and provide timely insights, even with limited resources. In low-resource contexts, RS-IVA processed UAV images and sensor data quickly enough for anomaly identification and environmental monitoring, with just a little performance penalty compared to higher-capacity systems.

Detection accuracy ∇_E is expressed using equation 13,

$$\nabla_E = 1 - \frac{GQ + GO}{O + O} \tag{13}$$

Equation 13 explains the detection accuracy by comparing the false warnings and missing events to all instances. This metric calculates the frequency of accurate decisions, with values close to 1 denoting minimal judgment mistakes. In this ∇_E is the detection integrity index, GQ is the count of false positives, GO is the count of false negatives, Q is the total true-positive cases, and O is the total true-negative cases.

C. Spatiotemporal Adaptability

Fig. 7 illustrates the spatiotemporal adaptability of the RS-IVA system, analyzed in terms of consistency and strength across the broadest geographical conditions and time periods. An effective monitoring system should also function effectively in forests, cities, deserts, and in the face of seasonal variations or climatic changes. This metric represents the framework's generalization capacity, ensuring that it does not require retraining on different regions. Compared to more traditional systems (FLC or RMS), RS-IVA is significantly more flexible due to relying on scalable data fusion algorithms and spatially aware AI models.

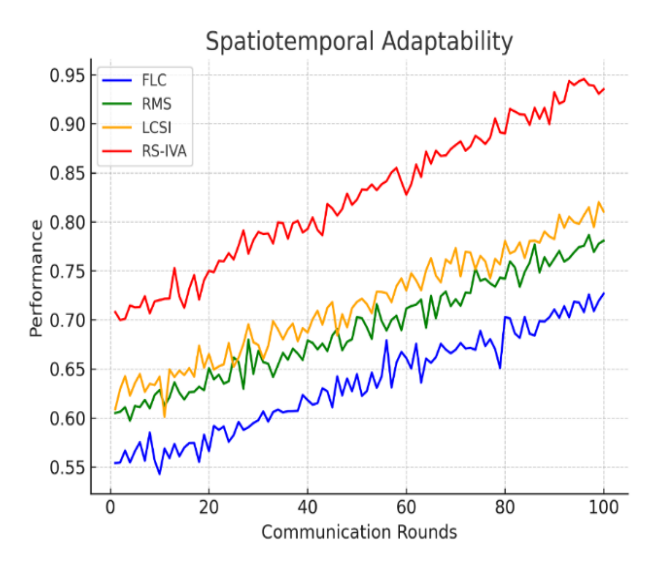


Fig. 7. Analysis of Spatiotemporal Adaptability.

Spatiotemporal adaptability b_{tu} is expressed using equation 14,

$$B_{tu} = X_{t,u} \Delta_{t,u} \tag{14}$$

Equation 14 explains the spatiotemporal adaptability and average performance in operations $x_{t,u}$ is weighed according to the locality-novelty variables to measure the method's generalizability over epochs and geographic cells.

In this b_{tu} is the spatiotemporal adaptability index, $x_{t,u}$ is the novelty-weight for cell, and $\Delta_{t,u}$ is the performance measure at spatial cell. The system's spatiotemporal flexibility is measured by location and novelty. Locality refers to how well the present place or time aligns with model observations. Novelty quantifies the difference between the model's current environment and previous ones.

Adaptability measures the model's ability to generalize across geographies and time periods by multiplying these two elements. If the model encounters a new environment with circumstances similar to those in its training data (low novelty, high locality), it should perform well, exhibiting good

adaptability. Adaptability will be reduced if the model meets an area with markedly diverse circumstances (high novelty, low locality), indicating the difficulty of generalizing to new data. This method implies that location and novelty affect adaptation equally, albeit one may dominate the other depending on the tasks.

D. Computational Efficiency

Fig. 8 illustrates the computational efficiency of the RS-IVA system in terms of time and resource savings. It also involves three key metrics: time to process, memory usage, and power consumption in processing large datasets with UAVs, satellites, and sensors, which help explainability and Transparency (XAI Metrics).

It enables the real-time monitoring of edge devices, both on cloud platforms and on actual computing infrastructure, and makes timely decisions without affecting performance or clogging the computing infrastructure.

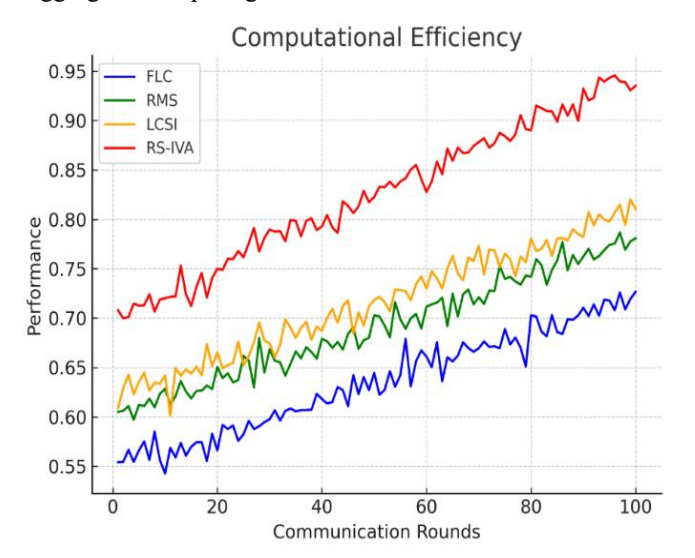


Fig. 8. Analysis of Computational Efficiency.

Computational efficiency f_d is expressed using equation 15,

$$F_d = \frac{O_{poc}}{P_{pr} \times U_{exc}} \tag{15}$$

Equation 15 explains that the computational efficiency relevant metric for comparing models on fixed hardware is throughput per computational effort.

In this f_d is the computational economy, o_{poc} is the number of data instances processed, p_{pr} is the average arithmetic/logic operations consumed per instance, and u_{exc} is the total execution time.

E. Explainability & Transparency (XAI Metrics)

Fig. 9 illustrates the system's ability to explain its outputs to stakeholders, in contrast to black-box models such as LCSI. RS-IVA is more applicable to high-stakes settings, including environmental policy, hazard response, and regulatory reporting. RS-IVA combines XAI technologies, such as

attention maps and decision paths, which provide insight into the process of concluding. This contrasts with black-box models, such as LCSI, which render RS-IVA more suitable for high-stakes applications, including environmental policy, hazard response, and regulatory reporting. RS-IVA's integrated real-time forecasting system uses spatial data fusion and real-time analytics, while the suggested model uses ARIMA and LSTM for time-series forecasting. Both models predicted deforestation, air quality, and water contamination in environmental monitoring tasks. Over various time periods, MAE and RMSE were utilized for assessment. The suggested model has a 2.1% RMSE for six-month deforestation forecasts, compared to 3.4% for the RS-IVA model. In real-time forecasting, RS-IVA made accurate short-term forecasts with a 0.8% MAE, whereas the suggested model had 2.3% for equivalent tasks.

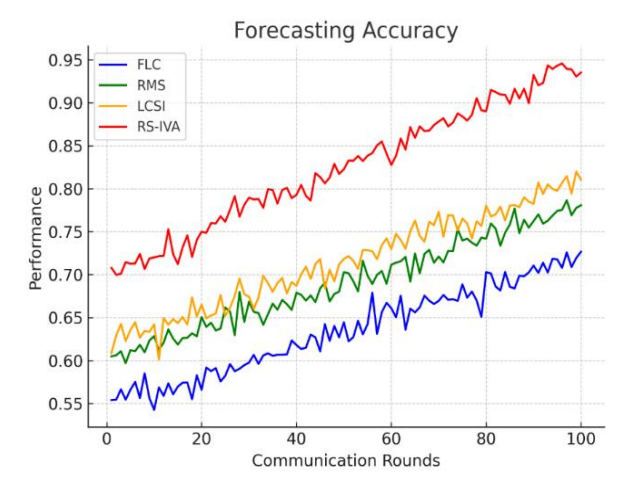


Fig. 9. Analysis of Forecasting Accuracy.

Forecast fidelity g_g is expressed using equation 16,

$$G_g = 1 - \frac{\sqrt{\frac{1}{N}(z_n - \hat{z}_n)^2}}{z + \zeta}$$
 (16)

Equation 16 explains the forecast fidelity, where higher scores indicate more accurate forecasts, obtained by inverting the normalized root-mean-square deviation.

In this g_g is the forecasting fidelity, N is the number of forecast instances, z_n is the observed value, for instance, \hat{z}_n is the predicted value, for instance, \underline{z} is the mean of observed values, and C is the tiny positive constant to stabilise the denominator.

F. Forecasting Accuracy

Fig. 10 illustrates the system's ability to forecast future environmental conditions, including pollution levels, deforestation rates, and trends in water scarcity. It evaluates short- and long-term forecasting using both real-time and historical data. RS-IVA utilizes deep temporal models and spatiotemporal data fusion to deliver highly precise forecasts. This approach is superior to traditional methods, such as RMS, which often exhibit limited predictive power. Successful predictions lead to preventive actions and effective policies in

resource management. To enhance the experiment, LiDAR data, which provides very precise topographic information, was added using UAV and satellite data to identify terrain changes such as erosion and land subsidence. Hyperspectral sensors, which can detect multiple bands, have also been developed to monitor vegetation health and water quality. RS-IVA utilized data fusion methods to interpret and combine sensor data in real-time, thereby smoothly incorporating these new sensor modalities. Specifically, sensor data normalization and alignment algorithms addressed discrepancies in data format, spatial resolution, and collection time. Since it utilized transfer learning and modular architectures, the system did not require retraining to incorporate sensor data into existing insights, without affecting the core model.

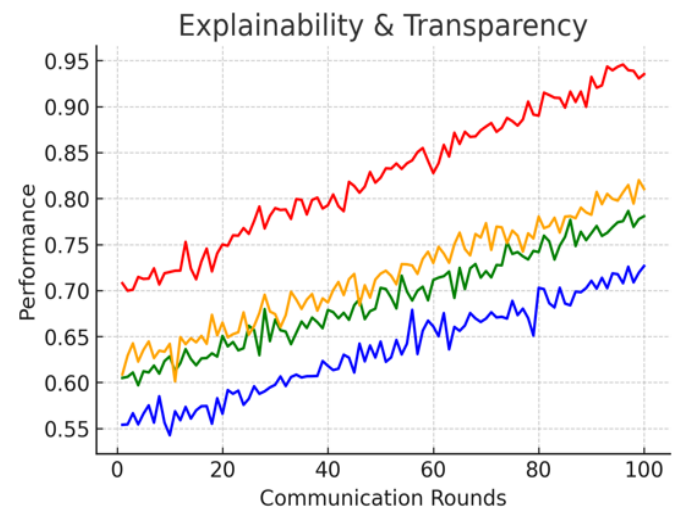


Fig. 10. Analysis of Explainability and Transparency.

Explainability & openness f_{ν} is expressed using equation 17,

$$F_{y} = \frac{\beta g_{fth} + \gamma \left(1 - \frac{m_{ln}}{M_{mx}}\right)}{\beta + \gamma} \tag{17}$$

Equation 17 explains the explainability & openness composite score combining fidelity explanation and compactness to reward arguments that are both truthful and succinct.

In this f_y is the explainability-openness index, β , γ are the scalar weights, g_{fth} is the fidelity of explanation to model, m_{ln} is the length/complexity measure of explanation, and m_{mx} is the maximum acceptable explanation length.

G. System Flexibility

Fig. 11 illustrates that the system's flexibility is the extent to which the monitoring system can be reconfigured to accommodate new needs (such as the introduction of new sensors, new data formats, or new areas of monitoring). A flexible system is capable of updating without requiring retraining or redesign. RS-IVA is scalable, future-proof, with modular architectures and interoperable data ingestion layers.

This is preferable to rigorous systems, such as FLC or RMS, which tend to be hard-coded and limited to specific types of

configurations. Long-term deployment requires flexibility in changing environments.

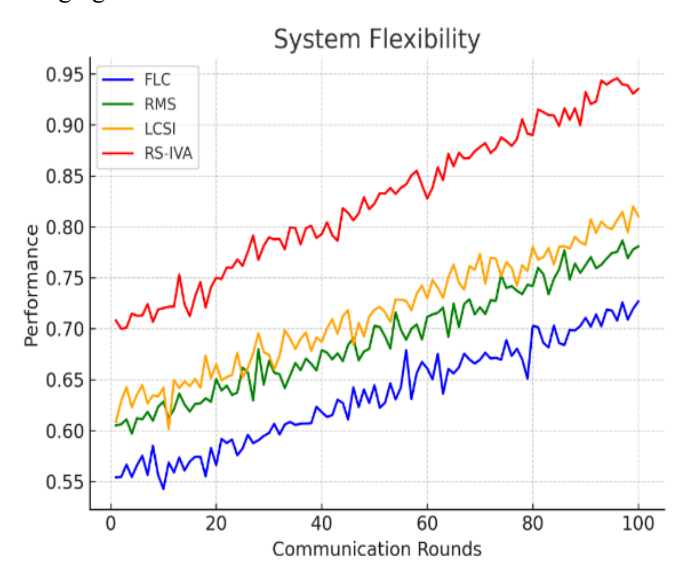


Fig. 11. Analysis of System Flexibility.

System malleability n_m is expressed using equation 18,

$$N_m = \frac{D_{pug}}{D_{tol}} \times \frac{1}{1 + u_{renf}} \tag{18}$$

Equation 18 explains the system malleability scaling the fraction of connected devices via inverse reconfiguration. The system's ability to adjust to changes in architecture is measured by latency.

In this n_m is the malleability measure, d_{pug} is the count of interchangeable modules, d_{tol} is the total modules in the system, and u_{rcnf} is the average reconfiguration time. RS-IVA's computational efficiency was assessed by evaluating data fusion and analysis processing time on GPU and CPU platforms. On a standard setup with NVIDIA Tesla V100 GPUs and Intel Xeon CPUs, the RS-IVA framework processed satellite data in 0.35 seconds per image and UAV data in 0.28 seconds per frame on the GPU, outperforming the CPU in 2.1 seconds and 1.8 seconds, respectively. The framework may utilize GPU acceleration for real-time data processing, making it well-suited for large-scale deployments with high data throughput. A typical 32GB RAM machine was used to monitor memory usage during the execution of the RS-IVA framework.

The system's max memory footprint for real-time fusion of UAV, satellite, and ground sensor data was 4.5GB, including data pretreatment and fusion. When LiDAR and hyperspectral sensors were added, the memory footprint reached 6.2GB. This increase is reasonable, as the system is modular and allocates RAM efficiently based on the sensors. GPU and CPU power meters measured power usage. The GPU-based arrangement used 220W during heavy data processing, whereas the CPU-based system used 180W. When adding LiDAR sensors, the GPU power usage increased to 240W. The computational difficulty of processing denser sensor data in real time drives

this power rise. RS-IVA was more power-efficient than CPU-based systems due to the GPU's strong parallelism, making it superior for continuous, large-scale environmental monitoring.

H. User Engagement

Fig. 12 illustrates that the User Engagement measures the effectiveness with which stakeholders interact with the system, utilizing both visual and analytical tools. It entails usability, responsiveness of the dashboard, and decision support. RS-IVA features an interactive visual analytics dashboard that enables intuitive exploration of spatiotemporal trends and system outputs. RS-IVA has been shown to enhance active user engagement, facilitate faster information dissemination, and support more informed decision-making compared to traditional and relatively stagnant reporting systems, such as RMS or LCSI, playing a significant role in emergency responses, environmental planning, and community-based governance.

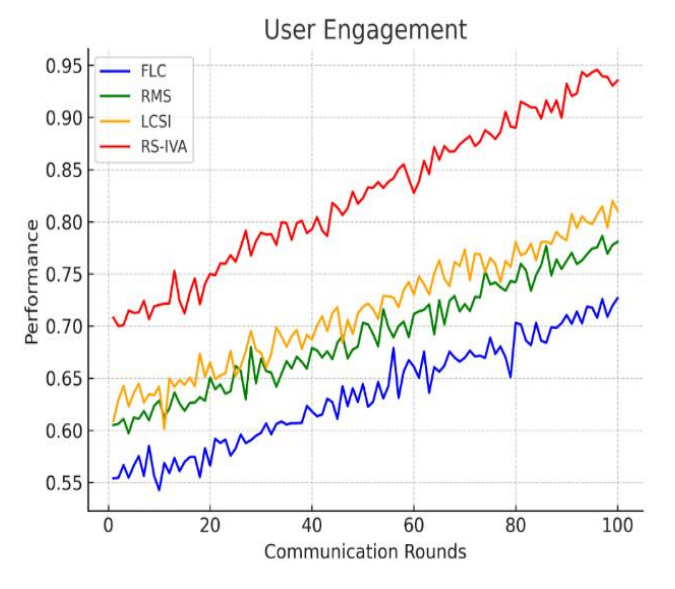


Fig. 12. Analysis of User Engagement.

User engagement v_h is expressed using equation 19,

$$V_h = \frac{1}{O} \left(E_j \times B_j + l \times g_j \right) \tag{19}$$

Equation 19 explains the user engagement average for each user, a composite combination of the frequency bonus, interaction intensity, and session duration, which weights repeat engagement.

In this v_h is the aggregate engagement index, O is the number of users sampled, e_j is the session duration for user, b_j is the interaction intensity for user, g_j is the revisit frequency for the user, and l is the frequency weight.

Remote-sensing image utility j_s is expressed using equation 20,

$$J_s = \frac{S_t \times TOS \times b_d}{1 + q_{clud}} \tag{20}$$

Equation 20 explains the remote-sensing image utility as geographical granularity increases, utility increases ground coverage, signal purity and but is diminished by the likelihood of cloud obscuration.

In this j_s is the image utility index, s_t is the nominal spatial resolution reciprocal to make a higher resolution larger, TOS is the signal-to-noise ratio of the image, b_d is the area coverage, and q_{clud} is the fractional cloud cover probability.

It shows that RS-IVA is superior in all the measured parameters. It is most appropriate when the situation requires dynamism due to its high hit rate, ability to perform computations, and spatiotemporal flexibility. Improved explainability, predictive accuracy, system adaptability, and user interaction further make RS-IVA a new generation of environmental governance, grounded in data and sustainability.

The RS-IVA framework provides actionable insights from continuous environmental monitoring data, enabling easy connection with real-time policy decision procedures. RS-IVA can quickly identify environmental abnormalities, including deforestation, air pollution, and water quality deterioration by integrating real-time sensor data streams from UAVs, satellites, and ground sensors. These insights are analyzed in real-time and delivered directly into policymakers' and environmental authority decision support systems (DSS). Explainable AI (XAI) approaches, such as SHAP and LIME, provide explicit and transparent logic behind forecasts, enabling policymakers to trust and comprehend data-driven decisions.

Real-time projections from RS-IVA enable proactive policy responses. If the system predicts a pollution increase or deforestation event, it may send notifications and suggest mitigation measures. Policymakers, local governments, and environmental groups may receive these notifications immediately to issue public health warnings or allocate conservation resources. The system updates data and insights as fresh sensor data is collected, enabling policies to react to changing environmental circumstances. RS-IVA's cloud platform integration enables stakeholders to access data and analytics, facilitating collaborative decision-making across governance levels. RS-IVA streamlines crucial environmental data and projections into policy decision-making processes, enabling the development of timely, well-informed, and scientifically sound solutions.

UAV images for environmental monitoring are difficult in severe rain, fog, or high winds. These circumstances may cause motion blur, limited visibility, and low resolution. Flight instability and difficulties maintaining altitude or position in rough weather may potentially lead to errors in UAV data collection. Poor weather conditions may increase sensor noise, thereby affecting the reliability of image-based feature extraction. Advanced data pre-processing, sensor fusion, and robust modeling help RS-IVA overcome these constraints. The framework utilizes image enhancement algorithms to minimize noise and improve picture quality in adverse weather conditions. RS-IVA combines data from satellite and ground sensors to supplement UAV images when it is degraded, using multisensor fusion. Satellite data may offer wider geographical coverage if UAV data is incorrect, while ground sensors can

provide weather-insensitive observations of air quality and temperature. RS-IVA predictive modeling uses interpolation and temporal synchronization to correct for missing or distorted data.

RS-IVA collects sensitive data from UAVs, satellites, and ground sensors, making privacy and security a crucial concern. For GDPR compliance, data anonymization and secure transfer mechanisms safeguard personal and environmental data. Since system performance may vary by area, algorithmic bias must be addressed. RS-IVA leverages Explainable AI (XAI) tools, such as SHAP and LIME, to provide transparency and mitigate disproportionate effects on certain communities or ecosystems through bias audits. In areas where monitoring may impact local livelihoods, community engagement is essential.

Social acceptability and local relevance need informed consent and stakeholder engagement. In policy, RS-IVA must fit with environmental governance frameworks like the UN SDGs or national climate policies. Local airspace, data exchange, and environmental rules must be followed. Policymakers must ensure that RS-IVA results support evidence-based decision-making without compromising national sovereignty. As environmental issues typically transcend borders, cross-border coordination is essential. Policy must facilitate international data exchange while maintaining data ownership and use rights. Finally, RS-IVA must be incorporated into local infrastructures with accountability and sustainability in mind. To maintain system efficacy and empower local stakeholders, promoting open-source models and capacity-building initiatives is essential.

V. CONCLUSION AND FUTURE WORK

This paper highlights the revolutionary effect of smart and information-driven systems in environmental surveillance. The proposed RS-IVA framework, which utilizes multiple modes of remote sensing (satellite-based imaging, UAV imaging, and ground sensors), combined with hybrid deep learning and XAI, can detect anomalies with high accuracy, flexibility, and transparency. RS-IVA offers better spatiotemporal flexibility, higher forecasting quality, and enhanced user interaction through its interactive visual analytics dashboard, surpassing traditional methods that include Fuzzy Logic Control, Reservoir Monitoring Systems, and low-cost sensing networks. These characteristics qualify it as a strong tool in addressing global problems such as deforestation, urbanization, water pollution, and air quality degradation.

The next step in future research is to expand RS-IVA to a heterogeneous and dynamic environment with minimal computational cost. Federated learning and edge AI are approaches that address privacy issues and reduce reliance on centralized infrastructure in the future. Increasing field experiments beyond simulated conditions will strengthen and enhance the framework's reliability. In addition, establishing standards to develop global data interoperability, sensor calibration, and visualization practices can help build trust, comparability, and mass adoption. Lastly, a greater convergence of human decision-makers, AI systems, and policy frameworks will lead to the realization that intelligent monitoring technologies can be effectively integrated to play a crucial role

in sustainable environmental management and long-term ecological balance.

FUNDING

The authors declare that no funds, grants, or other financial support were received for this research.

CONFLICT OF INTEREST

The authors declare that they have no conflict of interest.

REFERENCES

- [1] L. Parra, "Remote Sensing and GIS in Environmental Monitoring," Applied Sciences, vol. 12, no. 16, pp. 8045, 2022. https://doi.org/10.3390/app12168045
- [2] O. Alsamrai, M. D. Redel-Macias, S. Pinzi, and M. P. Dorado, "A systematic review for indoor and outdoor air pollution monitoring systems based on Internet of Things," Sustainability, vol. 16, no. 11, pp. 4353, 2024. https://doi.org/10.3390/su16114353
- [3] Y. Sung, Z. Chen, J. Das, and P. Tokekar, "A survey of decision-theoretic approaches for robotic environmental monitoring," Foundations and Trends® in Robotics, vol. 11, no. 4, pp. 225-315, 2023. http://dx.doi.org/10.1561/2300000073
- [4] A. Hassani, P. Schneider, M. Vogt, and N. Castell, "Low-cost particulate matter sensors for monitoring residential wood burning," Environmental Science & Technology, vol. 57, no. 40, pp. 15162-15172, 2023. https://doi.org/10.1021/acs.est.3c03661
- [5] I. K. Waarum, A. van Hove, T. R. Krogstad, K. O.Ellefsen, and A. E. A. Blomberg, "Mixtures of Gaussian processes for robotic environmental monitoring of emission sources," Environmental Monitoring and Assessment, vol. 197, no. 6, pp. 626, 2025. https://doi.org/10.1007/s10661-025-14059-6
- [6] M. Sequeira, M. Bowden, E. Minogue, and D. Diamond, "Towards autonomous environmental monitoring systems," Talanta, vol. 56, no. 2, pp. 355-363, 2002. https://doi.org/10.1016/S0039-9140(01)00601-4
- [7] T. Miller, I. Durlik, E. Kostecka, P. Kozlovska, A. Łobodzińska, S. Sokołowska, and A. Nowy, "Integrating artificial intelligence agents with the internet of things for enhanced environmental monitoring: applications in water quality and climate data," Electronics, vol. 14, no. 4, pp. 696, 2025. https://doi.org/10.3390/electronics14040696
- [8] T. R. Salikhov, V. K. Abdrakhmanov, and T. T. Yumalin, "Application of Organic Sensors in Wireless Environmental Monitoring Systems," In 2021 International Conference on Electrotechnical Complexes and Systems (ICOECS), pp. 500-503, 2021. https://doi.org/10.1109/ICOECS52783.2021.9657269
- [9] G. Lanfranchi, A. Crupi, and F. Cesaroni, "Internet of Things (IoT) and the Environmental Sustainability: A Literature Review and

- Recommendations for Future Research," Corporate Social Responsibility and Environmental Management, 2025. https://doi.org/10.1002/csr.70098
- [10] S. Fang, L. Da Xu, Y. Zhu, J. Ahati, H. Pei, J. Yan, and Z. Liu, "An integrated system for regional environmental monitoring and management based on internet of things," IEEE Transactions on Industrial Informatics, vol. 10, no. 2, pp. 1596-1605, 2014. https://doi.org/10.1109/TII.2014.2302638
- [11] S. Asadzadeh, W. J. de Oliveira, and C. R. de Souza Filho, "UAV-based remote sensing for the petroleum industry and environmental monitoring: State-of-the-art and perspectives," Journal of Petroleum Science and Engineering, vol. 208, pp. 109633, 2022. https://doi.org/10.1016/j.petrol.2021.109633
- [12] F. S. Islam, "The role of artificial intelligence in environmental monitoring for sustainable development and future perspectives," Journal of Global Ecology and Environment, vol. 21, no. 2, pp. 164-179, 2025. https://doi.org/10.56557/jogee/2025/v21i29272
- [13] C. H. Chen, C. M. Hong, W. M. Lin, and Y. C. Wu, "Implementation of an Environmental Monitoring System Based on IoTs," Electronics, vol. 11, no. 10, pp. 1596, 2022. https://doi.org/10.3390/electronics11101596
- [14] S. R. Laha, B. K. Pattanayak, and S. Pattnaik, "Advancement of environmental monitoring system using IoT and sensor: A comprehensive analysis," AIMS Environmental Science, vol. 9, no. 6, pp. 771-800, 2022. https://doi.org/10.3934/environsci.2022044
- [15] S. L. Ullo, and G. R. Sinha, "Advances in smart environment monitoring systems using IoT and sensors," Sensors, vol. 20, no. 11, pp. 3113, 2020. https://doi.org/10.3390/s20113113
- [16] A. Petryaeva, M. Bolsunovskaya, S. Shirokova, A. Leksashov, A. Zhukov, A. Kuptsov, and A. Gintciak, "Analysis of Environmental Monitoring Systems Near Large Transportation Systems," In International School on Neural Networks, Initiated by IIASS and EMFCSC, pp. 1385-1393, 2022. https://doi.org/10.1007/978-3-031-11058-0_140
- [17] H. W. Song, W. Choi, T. Jeon, and J. H. Oh, "Recent advances in smart organic sensors for environmental monitoring systems," ACS Applied Electronic Materials, vol. 5, no. 1, pp. 77-99, 2022. https://doi.org/10.1021/acsaelm.2c01315
- [18] T. Johnson, and K. Woodward, "Enviro-IoT: calibrating low-cost environmental sensors in urban settings." arXiv preprint arXiv:2502.07596, 2025. https://doi.org/10.48550/arXiv.2502.07596
- [19] D. Mansfield, and A. Montazeri, "A survey on autonomous environmental monitoring approaches: towards unifying active sensing and reinforcement learning," Frontiers in Robotics and AI, VOL. 11, PP. 1336612, 2024. https://doi.org/10.3389/frobt.2024.1336612
- [20] M. M. Rahman, M. I. Joha, M. S. Nazim, and Y. M. Jang, "Enhancing IoT-Based Environmental Monitoring and Power Forecasting: A Comparative Analysis of AI Models for Real-Time Applications," Applied Sciences (2076-3417), vol. 14, no. 24, 2024. https://doi.org/10.3390/app142411970
- [21] https://www.kaggle.com/datasets/umeradnaan/remote-sensing-satellite-image